

# Precision Spectroscopy at Heavy Ion Ring Accelerator SIS300

Hartmut Backe

*Institut für Kernphysik, Johannes Gutenberg-Universität Mainz, D-55099 Mainz,  
Germany*

January 03, 2007

**Abstract.** Unique spectroscopic possibilities open up if a laser beam interacts with relativistic lithium-like ions stored in the heavy ion ring accelerator SIS300 at the future Facility for Antiproton and Ion Research FAIR in Darmstadt, Germany. At a relativistic factor  $\gamma = 36$  the  ${}^2P_{1/2}$  level can be excited from the  ${}^2S_{1/2}$  ground state for any element with frequency doubled dye-lasers in collinear geometry. Precise transition energy measurements can be performed if the fluorescence photons, boosted in forward direction into the X-ray region, are energetically analyzed with a single crystal monochromator. The hyperfine structure can be investigated at the  ${}^2P_{1/2} - {}^2S_{1/2}$  transition for all elements and at the  ${}^2P_{3/2} - {}^2S_{1/2}$  transition for elements with  $Z \leq 50$ . Isotope shifts and nuclear moments can be measured with unprecedented precision, in principle even for only a few stored radioactive species with known nuclear spin. A superior relative line width in the order of  $5 \cdot 10^{-7}$  may be feasible after laser cooling, and even polarized external beams may be prepared by optical pumping.

**Keywords:** laser spectroscopy, relativistic lithium-like ions, laser cooling, hyperfine spectroscopy, nuclear polarization, SIS300

**Abbreviations:** FAIR – Facility for Antiproton and Ion Research; HI – Heavy Ion; QED – Quantum Electrodynamics; CCD – Charge Coupled Device; EBIT – Electron Beam Ion Trap

## 1. Introduction

The central part of the planned FAIR project in Darmstadt is a heavy ion synchrotron called SIS300 with a magnetic rigidity  $B\rho = 300$  Tm and a circumference of 1100 m [Gutbrod et al. 2006]<sup>1</sup>. The magnetic field will be produced by superconducting magnets with a maximum induction of 6 Tesla which can be ramped with a rate of 1 T/s. With this synchrotron bare uranium can be accelerated up to a maximum energy of 34 GeV/u, corresponding to a relativistic factor  $\gamma = 1/\sqrt{1 - \beta^2} = 37.5$  and a reduced velocity  $\beta = v/c = 0.9996444$ , with  $c$  the speed of light. A fascinating possibility of this accelerator is the excitation of few electron systems by the interaction with the light of conventional lasers

---

<sup>1</sup> The parameters used in this paper do not match exactly with the parameters of this report.



in a collinear geometry. If the laser beam counter-propagates lithium-like uranium with  $\gamma = 36$ , the laser light at the blue edge of the visible spectral range with an energy of  $\hbar\omega_L = 3.898$  eV is Doppler-shifted and appears in the rest frame of the Li-like system with an energy of  $\hbar\omega_0 \cong 2\gamma\hbar\omega_L = 280.6$  eV. As will be outlined in more detail in section 2 this is just the  ${}^2P_{1/2} - {}^2S_{1/2}$  transition energy in lithium-like uranium. A variety of spectroscopic possibilities exist if this transition can be induced. As will be pointed out in section 3 the combination with a precise single crystal X-ray spectrometer, which detects the fluorescence photons boosted in forward direction up to an energy of  $\hbar\omega_X = 2\gamma\hbar\omega_0 = 20.2$  keV allows both, very accurate measurements of the transition energy  $\hbar\omega_0$  and the relativistic factor  $\gamma$ . If radioactive Li-like ions could be injected into the SIS300, a hyperfine spectroscopy would be possible for radioactive species with nuclear spin  $I > 0$ , see section 4. A few remarks on laser cooling will be made in section 5. In section 6 the possibility of a nuclear polarization by optical pumping with circularly polarized laser light will briefly be touched on. The paper closes in section 7 with a conclusion.

The essential ideas of this paper were for the first time presented by the author of this paper in the year 2000 at GSI in Darmstadt [Backe 2000], see also Gutbrod et al. 2001.

## 2. The ${}^2P_{1/2,3/2} - {}^2S_{1/2}$ transitions in lithium-like uranium

The three electron, lithium-like level scheme of uranium is shown in figure 1. The third electron outside the closed  $1s^2$  shell is a  $2s$  electron, consequently the ground state is a  ${}^2S_{1/2}$  term. The lowest excited states belong to the  $1s^22p$  configuration and form  ${}^2P_{1/2}$  and  ${}^2P_{3/2}$  terms. The large fine-structure splitting of about 4.3 keV originates from relativistic effects.

A first precision measurement of the  ${}^2P_{1/2} - {}^2S_{1/2}$  transition energy of  $(280.59 \pm 0.09)$  eV was reported by Schweppe et al. 1991. The aim of this experiment was to test QED in few electron uranium. In a number of publications Lindgren et al., and Persson et al. calculated  $(280.52 \pm 0.28)$  eV which was in good agreement with the experiment. In the meantime better experiments by Brandau et al., who measured  $(280.516 \pm 0.099)$  eV, and by Beiersdorfer et al. were performed. In the latter reference a value of  $(280.645 \pm 0.015)$  eV is reported which was obtained with SuperEBIT. The accuracy of previous experiments was improved by nearly one order of magnitude. The best calculation of Yerokhin et al. 2001 without second order QED effects is  $(280.48 \pm 0.11)$  eV, and with inclusion of an estimated value of these effects

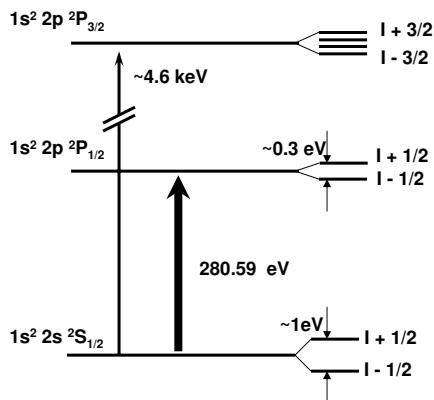


Figure 1. The lithium-like level scheme of uranium

( $280.64 \pm 0.21$ ) eV [Yerokhin 2005], i.e. the precision of the measurement exceeds currently the precision of the calculation by a factor of 14. Despite this situation a scheme is presented in the next section with which in future the experimental precision probably can be further improved by another factor of 4. Alternatively, it may be useful to measure  $\beta$  and  $\gamma$  of the Li-like ions with accuracies in the order of  $10^{-8}$  and  $10^{-5}$ , respectively, see subsection 3.6.

### 3. Precision transition energy measurement in Li-like uranium at SIS300

#### 3.1. PROPOSED EXPERIMENTAL SETUP

The proposed experimental setup is schematically shown in figure 2. A laser beam with a photon energy of 5.465 eV, corresponding to a vacuum wavelength  $\lambda = 226.87$  nm, counter-propagates in a straight section of SIS300 a Li-like uranium beam with a relativistic factor  $\gamma = 25.68$ . The photon energy in the rest frame of the Li-like  $U^{89+}$ -ion is

$$\hbar\omega_0 = \sqrt{\frac{1+\beta}{1-\beta}} \hbar\omega_L = 280.6 \text{ eV} \quad (1)$$

which is with  $\beta = \sqrt{1-1/\gamma^2} = 0.99924152$  just the  ${}^2P_{1/2} - {}^2S_{1/2}$  transition energy. De-excitation photons emitted in forward direction with respect to the Li-like uranium beam are boosted in the laboratory system to an energy

$$\hbar\omega_X = \sqrt{\frac{1+\beta}{1-\beta}} \hbar\omega_0 = 14.41 \text{ keV}. \quad (2)$$

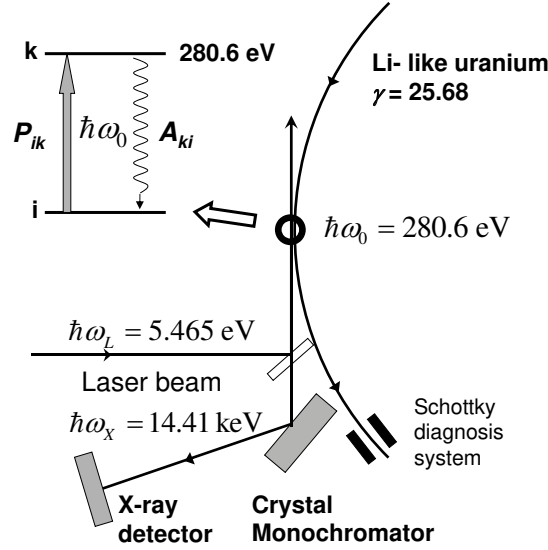


Figure 2. Proposed schematic experimental setup. The laser beam with photons of energy  $\hbar\omega_L$  is reflected by a thin mirror into a straight section of SIS300 and interacts in a collinear geometry with lithium-like uranium ions moving in opposite direction. De-excitation photons from the  ${}^2P_{1/2} - {}^2S_{1/2}$  transition with an energy  $\hbar\omega_0 = 280.6$  eV appear predominantly in forward direction with respect to the HI beam at an X-ray energy  $\hbar\omega_X = 14.41$  keV. The photon energy is measured by a single crystal monochromator.

Occurrence of X-rays indicates resonance absorption of laser photons in the Li-like system. However, for an accurate measurement of the transition energy  $\hbar\omega_0$  also the reduced velocity  $\beta$  or the relativistic factor  $\gamma$  must be known with high precision. This can be achieved by an energy measurement of the X-ray photons with the aid of a single crystal monochromator. In this manner, two very precise experimental methods are combined. The laser photon energy can be determined easily with a relative accuracy of  $5 \cdot 10^{-7}$  and the X-ray energy with  $2.8 \cdot 10^{-5}$ , see subsection 3.6. Combining equations (1) and (2), the transition energy  $\hbar\omega_0$ , the reduced velocity  $\beta$ , and the the relativistic factor  $\gamma$  of the Li-like uranium ion can be determined:

$$\hbar\omega_0 = \sqrt{\hbar\omega_X \cdot \hbar\omega_L}, \quad (3)$$

$$\beta = \frac{\hbar\omega_X/\hbar\omega_L - 1}{\hbar\omega_X/\hbar\omega_L + 1}, \quad (4)$$

$$\gamma = \frac{1}{2} \frac{\hbar\omega_X/\hbar\omega_L + 1}{\sqrt{\hbar\omega_X/\hbar\omega_L}} \cong \frac{1}{2} \sqrt{\frac{\hbar\omega_X}{\hbar\omega_L}}. \quad (5)$$

The relative accuracies of a measurement of  $\beta$  and  $\gamma$  are  $\Delta\beta/\beta = 2.1 \cdot 10^{-8}$  and  $\Delta\gamma/\gamma = 1.4 \cdot 10^{-5}$ , respectively, see also subsection 3.6.<sup>2</sup>

### 3.2. ANGULAR DISTRIBUTION AND PHOTON ENERGY IN THE LABORATORY SYSTEM

In reality the photons are emitted in the rest frame of the Li-like ion with an angular distribution which will be assumed to be isotropic, i.e.  $d\dot{n}_0/d\Omega_0 = \dot{n}_0/(4\pi)$ . The angular distribution in the laboratory frame is given by

$$\frac{d\dot{n}}{d\Omega} = \frac{d\dot{n}_0}{d\Omega_0} \frac{d\Omega_0}{d\Omega} \frac{dt_0}{dt}, \quad (6)$$

$$\frac{d\Omega_0}{d\Omega} = \frac{1}{\gamma^2(1 - \beta \cdot \cos \Theta)^2}, \quad (7)$$

$$\frac{dt_0}{dt} = \frac{1}{\gamma} \quad (8)$$

with  $d\Omega_0/d\Omega$  the relativistically transformed solid angle ratio which follows from the relation

$$\cos \Theta_0 = \frac{\cos \Theta - \beta}{1 - \beta \cos \Theta}. \quad (9)$$

Here  $\Theta_0$  and  $\Theta$  are the observation angles with respect to the velocity vector  $\mathbf{v}$  of an individual Li-like ion in the rest frame of the Li-like ion and the laboratory frame, respectively. Further on,  $dt_0/dt = 1/\gamma$  is the relativistic time dilatation<sup>3</sup>. The transition energy in the rest frame of the Li-like system is

$$\hbar\omega_0 = \gamma(1 + \beta \cos \Psi)\hbar\omega_L \quad (10)$$

with  $\Psi$  the angle which an individual ion with the velocity vector  $\mathbf{v}$  makes with the laser beam axis. In the small angle approximation, with  $\vec{\theta}$  the observation angle with respect to the nominal velocity vector  $\mathbf{v}_0$  of the Li-like ion beam and  $\vec{\psi}$  the angular deviation of an individual

<sup>2</sup> It should be mentioned that the precision of the X-ray energy measurement and also the current value of the  ${}^2P_{1/2} - {}^2S_{1/2}$  transition energy  $\hbar\omega_0$  is not high enough for an improved test of the time dilatation in special relativity. Such a test is based on equation (3) which can be rewritten with a small additional term as  $\hbar\omega_L \cdot \hbar\omega_X/\hbar\omega_0^2 = 1 + 2\hat{\alpha}(\beta^2 + \dots)$ . The upper limit of the parameter  $\hat{\alpha}$  is currently  $\hat{\alpha} < 2.2 \cdot 10^{-7}$ , see Saathoff et al. 2003. An improvement of this value would require a measurement of  $\hbar\omega_L$ ,  $\hbar\omega_X$ , and  $\hbar\omega_0$  with at least an accuracy of  $10^{-7}$ .

<sup>3</sup> For a nice survey of relevant formulas of Lorentz transformation in storage rings see Habs et al. 1991, and Schramm et al. 2004

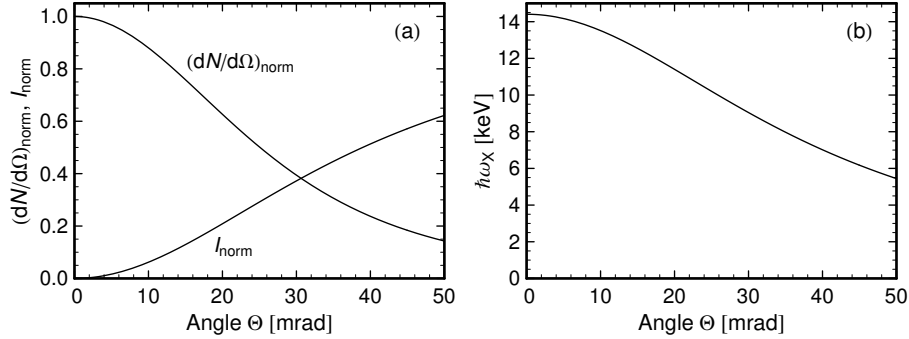


Figure 3. (a) Angular distribution  $(dN/d\Omega)_{norm}$  and integrated intensity  $I_{norm} = \int_0^\Theta (dN/d\Omega)d\Omega/(4\pi)$ , and (b) X-ray energy  $\hbar\omega_X$ , both as function of the observation angle  $\Theta$  in the laboratory system for  $\Psi = 0$ . The angular distribution  $(dN/d\Omega)_{norm}$  is normalized to its value at  $\Theta = 0$ ,  $I_{norm}$  approaches 1 for  $\Theta \rightarrow \pi$ .

ion from  $\mathbf{v}_0$ , the photon energy is

$$\hbar\omega_X = \frac{\hbar\omega_0}{\gamma(1 - \beta \cdot \cos|\vec{\theta} - \vec{\psi}|)} \cong \frac{2\gamma}{1 + (|\vec{\theta} - \vec{\psi}|\gamma)^2} \hbar\omega_0, \quad (11)$$

with  $\hbar\omega_0$  the photon energy in the Li-like system. From equations (10) and (11) the relation

$$\hbar\omega_X = \frac{1 + \beta \cos \psi}{1 - \beta \cdot \cos|\vec{\theta} - \vec{\psi}|} \hbar\omega_L \cong \frac{4\gamma^2}{1 + (|\vec{\theta} - \vec{\psi}|\gamma)^2} \hbar\omega_L. \quad (12)$$

follows which directly relates the laser photon energy  $\hbar\omega_L$  to the X-ray energy  $\hbar\omega_X$ .

Angular distribution  $dN/d\Omega$ , integrated intensity  $\int_0^\Theta (dN/d\Omega)d\Omega$  and X-ray energy  $\hbar\omega_X$  are shown in fig. 3 (a) and (b) as function of the observation angle  $\Theta$ . It is worthwhile to notice that in a cone with a polar angle  $\Theta = 50$  mrad, corresponding to  $2.86^\circ$  only, already more than 60 % of the intensity is concentrated.

### 3.3. THE LASER SYSTEM AND FLUORESCENCE RATE ESTIMATE

Laser light with a wavelength of  $\lambda = 226.9$  nm can be produced by an Excimer laser running on XeF (351/353 nm) which pumps a dye laser, for example. The output of the latter must be frequency doubled by a BBO crystal. Assuming a mean output power of the Excimer laser  $\bar{P} = 250$  W at a repetition rate  $f_{rep} = 10$  kHz and a pulse width of  $\Delta t_{pulse} = 10$  ns, the instantaneous pulse power output of the frequency doubled laser may amount to 50 kW. A bandwidth of the dye laser radiation  $\Delta\nu_D \simeq 1$  GHz can be reached by means of an intracavity etalon which

may further be reduced in the frequency doubling unit to  $\Delta\nu_L \simeq 0.7$  GHz or  $\Delta\nu_L/\nu_L \simeq 5.3 \cdot 10^{-7}$ . With these numbers the spectral photon flux within a single laser pulse amounts to  $\Delta\dot{N}_{pulse}/(\Delta\nu_L/\nu_L) \simeq 1.1 \cdot 10^{29}/\text{s}$ .

A lifetime of  $61.8 \pm 1.2(\text{stat}) \pm 1.3(\text{syst})$  ps of the  $2p \ ^2P_{1/2}$  has been measured by Schweppe et al. which corresponds to a transition rate  $A_{ki} = 1.62 \cdot 10^{10}/\text{s}$  or a relative level width  $\Gamma/\hbar\omega_0 = 0.38 \cdot 10^{-7}$ . This width is small in comparison to the relative band width of the photon flux in the rest frame of the Li-like ion  $\Delta\hbar\omega_0/\hbar\omega_0 = \Delta\nu_L/\nu_L = 5.3 \cdot 10^{-7}$ . Under these circumstances the induced transition rate is given by the equation

$$P_{ik} = \frac{d^2 \dot{N}_{pulse}^0}{dA \cdot d\hbar\omega_0/\hbar\omega_0} A_{ki} \frac{g_k}{g_i} \frac{\pi^2}{c} \left( \frac{\hbar c}{\hbar\omega_0} \right)^3, \quad (13)$$

with  $g_k$  and  $g_i$  the statistical weights. At a cross-section  $A = 10 \text{ mm}^2$  of the laser beam in the interaction region, the photon flux in the rest frame of the Li-like ion is  $d^2 \dot{N}_{pulse}^0/(dA \cdot d\hbar\omega_0/\hbar\omega_0) = \gamma \cdot d^2 \dot{N}_{pulse}/(dA \cdot d\nu_L/\nu_L) = \gamma \cdot 1.1 \cdot 10^{28}/(\text{mm}^2\text{s})$ . The number of induced transitions in a laser pulse of duration  $\Delta t_{pulse} = 10 \text{ ns}$  is, with  $P_{ik}$  of equation (13),  $P_{ik} \Delta t_{pulse}^0 = P_{ik} \Delta t_{pulse}/\gamma = 20.4$ , with  $\Delta t_{pulse}^0$  the pulse length in the rest frame of the Li-like system. This number is much larger as the spontaneous transition rate  $A_{ki} \Delta t_{pulse}/\gamma = 6.3$ , meaning that the effect of saturation must be taken into account. In the following all estimations of the spontaneous transition rates are performed in the saturation limit, since the experimental conditions are close to saturation. The number of emitted photons per laser pulse and per lithium-like uranium ion is then

$$N_{0,sat} = \frac{1}{2} \left( A_{ki} \frac{\Delta t_{pulse}}{\gamma} + 1 \right) = 3.7. \quad (14)$$

The additional summand 1 in the brackets originates from the fact that at saturation the Li-like ion is left with 50% probability in the excited state after the laser pulse has been past.

### 3.4. THE SINGLE CRYSTAL MONOCHROMATOR

The monochromator is shown in figure 4. A bent silicon single crystal with its surface cut parallel to the (220) crystal planes acts as a cylindrical mirror for the X-rays. It is energy dispersive in the horizontal direction. The deviation  $\varepsilon$  of the photon energy from the nominal Bragg energy, defined by the equation  $\hbar\omega_X = \hbar\omega_B(1 + \varepsilon)$ , with

$$\hbar\omega_B = \frac{2\pi\sqrt{h^2 + k^2 + l^2}}{a_0} \frac{\hbar c}{2 \sin \Theta_B}, \quad (15)$$

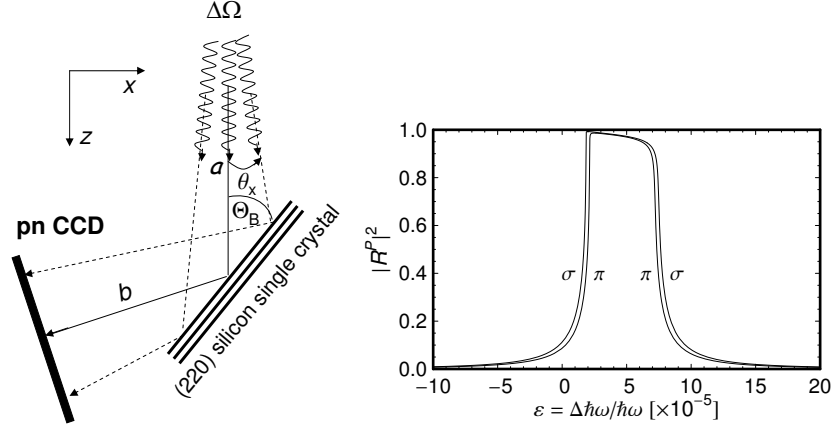


Figure 4. Scheme of the monochromator (left), and reflecting power ratios for  $\pi$  and  $\sigma$  polarized X-rays at  $\theta_x = 0$  (right). Dielectric susceptibilities  $\chi'_0 = -0.4677610^{-5}$ ,  $\chi''_0 = -0.3477710^{-7}$ ,  $\chi'_H = -0.2819110^{-5}$ ,  $\chi''_H = -0.3336410^{-7}$  were used in the calculation. A pn-CCD detector serves as a position sensitive and energy dispersive detector.

is approximately given by the expression [Caticha 1989]

$$\varepsilon = \frac{\chi'_0}{2 \sin^2 \Theta_B} - \frac{\theta_x}{\tan \Theta_B}. \quad (16)$$

Here  $\theta_x = \Theta - \Theta_B$  is the horizontal deviation from the nominal Bragg angle  $\Theta_B$ . The integers  $h, k, l$  are the Miller indices,  $a_0 = 5.4309 \text{ \AA}$  the lattice constant, and  $\chi'_0$  the real part of the mean dielectric susceptibility  $\chi_0 = \chi'_0 + i\chi''_0$ . The Bragg angle for  $\hbar\omega_B = 14.413 \text{ keV}$  amounts for the (220) reflection to  $\Theta_B = 12.944^\circ$ .

The finite energy width of the Bragg reflection can be calculated from the reflecting power ratio  $|R^P|^2$  with the amplitude ratio given by [Caticha 1989, Eq. (3.2)]

$$R^P(\theta_x, \varepsilon) = -y_P(u) + \text{sign}[\Re(y_P(u))] \sqrt{y_P^2(u) - 1} \quad (17)$$

$$y_P(u) = \frac{u + i\chi''_0}{P\chi_H} \quad (18)$$

$$u = 2 \sin^2 \Theta_B \left[ \left(1 - \frac{a}{R \cdot \sin \Theta_B}\right) \frac{\theta_x}{\tan \Theta_B} + \varepsilon \right] + \chi'_0. \quad (19)$$

The quantity  $\chi_H = \chi'_H + i\chi''_H$  is the Fourier component of the dielectric susceptibility of the analyzer crystal for the reciprocal lattice vector  $\mathbf{H}$ ,  $R$  the bending radius of the crystal, and  $P$  the polarization factor. The latter is  $P = \cos 2\theta_B$  for  $\pi$  polarization, with the polarization vector in the reflection plane, and  $P = 1$  for  $\sigma$  polarization, with the polarization

vector perpendicular to the reflection plane. Corresponding reflecting power ratios are shown in figure 4. Parameters for  $\chi_0$  and  $\chi_H$  were taken from Stepanov 1997.

The energy width of the Bragg reflection is in a good approximation given by the solution of equation (19) for  $\theta_x = 0$  with  $u-\chi'_0 = \pm|P||\chi_H|$ , i.e. the relative energy width is  $\Delta\varepsilon = \Delta\hbar\omega_X/\hbar\omega_X = |P||\chi_h|/\sin^2\Theta_B$ . With the energy deviation  $\varepsilon = -(\theta\gamma)^2$  of the emitted X-rays as function of the emission angle  $\vec{\theta} = \mathbf{e}_x\theta_x + \mathbf{e}_y\theta_y$ , which follows from equation (12) for  $\psi = 0$ , one obtains from equation (19) a quadratic equation

$$\theta_x^2 + \theta_y^2 \pm \left(1 - \frac{a}{R \cdot \sin \Theta_B}\right) \frac{\theta_x}{\gamma^2 \tan \Theta_B} - \frac{|P||\chi_h|}{2\gamma^2 \sin^2 \Theta_B} = 0 \quad (20)$$

the solution of which describes the accepted angular region. For a bending radius  $R$  chosen such that  $1 - a/(R \sin \Theta_B) = 0$  is fulfilled, the accepted angles  $\theta_x$  and  $\theta_y$  are located within a circle of radius  $\sqrt{|P||\chi_H|/(2\gamma^2 \sin^2 \Theta_B)}$  and the accepted solid angle is just  $\Delta\Omega^P = \pi|P||\chi_H|/(2\gamma^2 \sin^2 \Theta_B)$ . The corresponding solid angle in the rest frame of the Li-like system is  $\Delta\Omega_0^P = 4\gamma^2\Delta\Omega^P$ . The sum of both polarization states, normalized to  $4\pi$ , is

$$\frac{\Delta\Omega_0}{4\pi} = \frac{(1 + |\cos 2\Theta_B|)|\chi_H|}{4 \sin^2 \Theta_B} . \quad (21)$$

With  $|\chi_H| = 0.282 \cdot 10^{-5}$  [Stepanov 1997] the result is  $\Delta\Omega_0/4\pi = 2.67 \cdot 10^{-5}$ . The expected count rate at the pn-CCD detector is at saturation with  $n_0 = A_{ki}/2$

$$\dot{n} = \frac{1}{2} \frac{A_{ki}}{\gamma} \frac{(1 + |\cos 2\Theta_B|)|\chi_h|}{4 \sin^2 \Theta_B} . \quad (22)$$

It should be mentioned that the focal length of the cylindrical monochromator crystal amounts to  $f = (R/2) \sin \Theta_B$  which reduces with  $1 - a/(R \sin \Theta_B) = 0$  to  $f = a/2$ . It follows from the image equation  $1/a + 1/b = 1/f$  that at  $a = b$  the focus at the pn-CCD detector is just a vertical line.

### 3.5. COUNT RATE ESTIMATE

The detected X-ray rate at the pn-CCD detector is given by the equation

$$\dot{N}_X = \frac{\Delta\nu_L/\nu_L}{\Delta\gamma_b/\gamma} f_{rep} \cdot N_{Li} \cdot N_{0,sat} \frac{\Delta\Omega_0}{4\pi} \varepsilon_X . \quad (23)$$

The first factor is the fraction  $(\Delta\gamma_L/\gamma)/(\Delta\gamma_b/\gamma)$  of Li-like ions in a bunch which can be pumped. With  $\Delta\gamma_L/\gamma = \Delta\nu_L/\nu_L$  which follows

from equation (10) for  $\Delta\hbar\omega_0 = 0$ , it is given by the overlap of the relative laser bandwidth  $\Delta\nu_L/\nu_L = 5.3 \cdot 10^{-7}$  with the relative energy spread  $\Delta\gamma_b/\gamma = 10^{-4}$  of the Li-like ions in a bunch. A reduction due to the angular spread  $\sigma'_{HI}$  of the Li-like beam can be neglected as long as  $\sigma'_{HI} \ll 2\sqrt{\Delta\nu_L/\nu_L} = 1.46$  mrad holds. This latter relation can also be derived from the Doppler-shift formula (10) for which a first order expansion in  $\hbar\omega_L$  and a second order expansion in  $\Psi$  results in  $\Delta\Psi = 2\sqrt{\Delta\hbar\omega_L/\hbar\omega_L} = 2\sqrt{\Delta\nu_L/\nu_L}$  for  $\Delta\hbar\omega_0 = 0$ . In addition are  $f_{rep} = 10^4$ /s the laser repetition rate, which must be synchronized with a circulating bunch,  $N_{Li} = 10^5$  the number of Li-like ions in a bunch,  $N_{0,sat} = 3.7$ , and  $\Delta\Omega_0/4\pi = 2.67 \cdot 10^{-5}$ . The overall efficiency  $\varepsilon_X = 0.2$  takes into account the photon detection efficiency of the pn CCD as well as photon absorption in the window of the SIS300 vacuum chamber and the mirror for the laser light. The result for the count rate according to equation (23) is  $\dot{N}_X = 104$ /s which looks quite reasonable.

### 3.6. PRECISION OF ENERGY MEASUREMENT

The relative accuracy of a measurement of the  ${}^2P_{1/2} - {}^2S_{1/2}$  transition energy is, according to equation (3), given by

$$\frac{\Delta\hbar\omega_0}{\hbar\omega_0} = \frac{1}{2} \sqrt{\left(\frac{\Delta\hbar\omega_L}{\hbar\omega_L}\right)^2 + \left(\frac{\Delta\hbar\omega_X}{\hbar\omega_X}\right)^2}. \quad (24)$$

The precision of the X-ray energy measurement has two contributions. One is a sort of statistical error which is assumed to be 30 % of the half width of the Bragg reflex, i.e.,  $\delta\hbar\omega_X/\hbar\omega_X \simeq 0.3|\chi_H|/\sin^2\Theta_B = 1.7 \cdot 10^{-5}$ , with  $|\chi_H|/\sin^2\Theta_B = 5.6 \cdot 10^{-5}$ . The other one is a systematical error which originates from the energy calibration. Let us assume that the calibration is performed with the 14.41302(32) keV line of a  ${}^{57}\text{Co}$  ( $t_{1/2} = 271$  d) source which for this purpose must be placed temporarily in the interaction region of laser and Li-like ion beam. The relative precision  $\delta\hbar\omega_{14.4}/\hbar\omega_{14.4} = 2.2 \cdot 10^{-5}$  is of the same order of magnitude as the X-ray energy measurement. Since the error of the laser frequency measurement can be neglected, the total expected relative error of the  ${}^2P_{1/2} - {}^2S_{1/2}$  transition energy is  $\Delta\hbar\omega_0/\hbar\omega_0 = 1.4 \cdot 10^{-5}$  or  $\Delta\hbar\omega_0 = 0.0039$  eV. The latter would be a factor of about 4 better as the above quoted value of Beiersdorfer et al. 2005.

According to equation (5) the relativistic factor  $\gamma$  can be measured simultaneously with the same relative precision  $\Delta\gamma/\gamma = 1.4 \cdot 10^{-5}$ . It should be mentioned that the relative accuracy of  $\beta$  is  $\Delta\beta/\beta = 2.1 \cdot 10^{-8}$  because of  $\Delta\beta/\beta = (\Delta\gamma/\gamma)/(\beta\gamma)^2$  which follows from  $\gamma = 1/\sqrt{1 - \beta^2}$ .

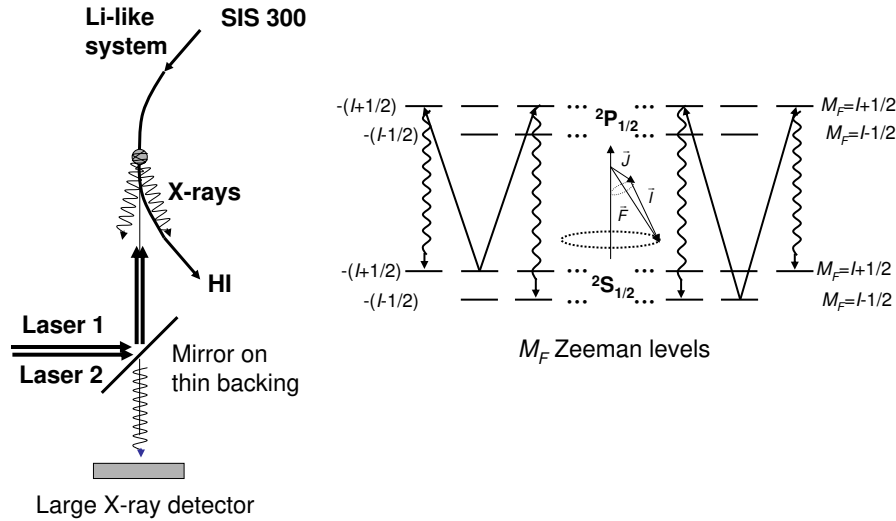


Figure 5. Scheme of the experimental setup for a measurement of the hyperfine structure (left), and pumping scheme (right). Shown are the Zeeman levels of the ground and excited state with  $F = I \pm 1/2$  the total angular momentum quantum numbers, and  $I$  the nuclear spin. While induced laser transitions can populate at resonance only one excited hyperfine level, radiative (downward) transitions can populate both ground state hyperfine levels. For clarity, not all possible transitions are drawn in.

#### 4. Hyperfine spectroscopy

If the nuclear spin  $I$  is not zero, ground and excited states of Li-like ions exhibit a hyperfine splitting. The  $^2S_{1/2}$  and the  $^2P_{1/2}$  states are split only by the magnetic hyperfine interaction while for the  $^2P_{3/2}$  also the quadrupole interaction contributes. The hyperfine splitting of the  $^2S_{1/2}$  ground-state is typically in the order of 0.5 eV [see, e.g., Shabaev et al. 1998, or Boucard et al. 2000]. It will be shown in the following that a hyperfine structure of the  $^2P_{1/2} - ^2S_{1/2}$  or even the  $^2P_{3/2} - ^2S_{1/2}$  transition can be investigated by laser spectroscopy as well.

The experimental setup is depicted in figure 5. It might be advantageous to use two laser beams, one pumping, e.g., the  $F_g = I - 1/2 \rightarrow F_e = I + 1/2$  transition, and the other the  $F_g = I + 1/2 \rightarrow F_e = I + 1/2$  one. Otherwise the signal may cease rapidly because of depopulation pumping. The relative line width  $\Delta\hbar\omega_0/\hbar\omega_0 = \Delta\gamma_b/\gamma$  of a transition is entirely determined by the energy distribution of the Li-like ions in a bunch which is in the order of  $\Delta\gamma_b/\gamma = 10^{-4}$ . Therefore, a line width  $\Delta\hbar\omega_0 \simeq 0.03$  eV is expected which may be small enough to resolve the hyperfine pattern.

Since in such an experiment only small relative energy changes of the hyperfine components must be measured, a high resolution X-ray detector is not required. A large area detector placed in forward direction can be used. This has the advantage that the accepted solid angle can be increased by a large factor, see figure 3. For an accepted polar angle of  $\Theta = 4$  mrad only, the relative accepted solid angle in the rest frame of the Li-like system is  $\Delta\Omega_0/(4\pi) = 0.0104$ , i.e., in the order of 1 %. Consequently, the count rate is expected to be rather high. Indeed, with  $(\Delta\nu_L/\nu_L)/(\Delta\gamma_b/\gamma) = 5.3 \cdot 10^{-3}$ ,  $f_{rep} = 10^4/\text{s}$ ,  $N_{Li} = 1$ ,  $N_{0,sat} = 3.7$ ,  $\Delta\Omega_0/(4\pi) = 0.0104$ , and  $\varepsilon_X = 0.5$  the count rate is according to equation (23)  $\dot{N}_X = 1.0/\text{s}$ . Notice, that in principle only one stored ion is required for the envisaged hyperfine spectroscopy! However, it is not at all clear that the X-ray detector may be located in forward direction because of expected excess background count rates. But even if a deflection of the X-ray beam out of the forward direction is necessary, e.g., by a pyrolytic graphite crystal which accepts a much larger bandwidth as a single crystal monochromator, the count rate may be sufficiently large with a few tens of Li-like ions in a bunch. Alternatively, the frequency of the pulse laser may be increased. Thereby the event rate increases linearly until the circulation frequency of the ions in the ring of about 275 kHz has been reached. It might also be sufficient to pump only with one laser beam and allow for depopulation pumping if the count rate is high enough.

This kind of hyperfine spectroscopy at Li-like ions has a number of advantages. First of all, hyperfine fields can be calculated with a very high accuracy, at least with a much better accuracy as for neutral atoms which is typically 10 % for the isotope shift and 3 % for hyperfine fields. This fact is of great importance since relative measurements can be avoided allowing a direct access to the Bohr-Weisskopf effect. Secondly, isotope shifts and magnetic hyperfine splittings can be measured for any element via the  $^2P_{1/2} - ^2S_{1/2}$  transition. At the highest relativistic factor  $\gamma = 36$  even a quadrupole interaction can be studied via the  $^2P_{3/2} - ^2S_{1/2}$  transition for all elements with  $Z \leq 50$ . (For the  $2s \ ^2S_{1/2} - 2p \ ^2P_{1/2,3/2}$  transition energies see Bosselmann et al. 1999, or Johnson et al. 1998.) Finally, it should be mentioned once more that the sensitivity is very high and only a very few or even only one radioactive ion may already be sufficient for the spectroscopy. However, such experiments would require a re-injection of radioactive species, produced by fragmentation reactions, into SIS300 as Li-like ions.

## 5. Laser cooling

The line width of the hyperfine components can be improved by several orders of magnitude by laser cooling as will be demonstrated in the following.<sup>4</sup> Momentum can be transferred to the Li-like ion by absorption of a laser photon as well as by re-emission of the X-ray. While the former momentum transfer is only  $\hbar\omega_L/c$ , the latter is according to equation (12) in the order  $\gamma^2\hbar\omega_L/c$  since the angular distribution of the X-rays is strongly peaked into forward direction, see subsection 3.2. The mean longitudinal momentum transfer in the laboratory system due to absorption and emission of a photon of energy  $\hbar\omega_0$  in the rest frame of the Li-like system is in the laboratory frame given by

$$\begin{aligned}\overline{\delta p_{\parallel}} &= \frac{\hbar\omega_L}{c} + \int \frac{(\hbar\omega_0/c) \cos \Theta}{\gamma(1 - \beta \cos \Theta)} \cdot \frac{f(\cos \Theta_0)}{4\pi} \cdot d\Omega_0 = \\ &= \frac{\hbar\omega_L}{c} + \int_{-1}^1 \frac{(\hbar\omega_0/c) \cos \Theta}{\gamma(1 - \beta \cos \Theta)} \cdot \frac{d(\cos \Theta)}{2\gamma^2(1 - \beta \cos \Theta)^2} = \quad (25) \\ &= \frac{\hbar\omega_L}{c} + \beta\gamma \frac{\hbar\omega_0}{c} = \gamma \frac{\hbar\omega_0}{c} . \quad (26)\end{aligned}$$

Here  $(\hbar\omega_0/c) \cos \Theta / (\gamma(1 - \beta \cos \Theta))$  is the longitudinal momentum transfer to the Li-like ion in the laboratory system by emission of a photon of momentum  $\hbar\omega_0/c$  in the rest frame of the ion. This relation follows from equation (11) for  $\vec{\psi} = 0$  and  $\theta = \Theta$  after division by  $c$ , which transforms the photon energy into the photon momentum, and the projection of the momentum on the velocity axis of the Li-like ion. The function  $f(\cos \Theta_0) = 1$  represents the angular distribution of the photon in the rest frame of the Li-like ion which is assumed to be isotropic. In equation (25) the solid angle is transformed by means of equation (7) into the laboratory system in which the integration is carried out. The integral of equation (25) can be solved analytically. The final result on the right hand side of equation (26) has been obtained with equation (10) for  $\Psi = 0$  after appropriate reshaping<sup>5</sup>. The instantaneous cooling force is in the laboratory system at saturation  $F_{\parallel} = dp_{\parallel}/dt = \overline{\delta p_{\parallel}} \cdot (1/2) \cdot A_{ki}/\gamma = (1/2) \cdot A_{ki} \cdot \hbar\omega_0/c$ .

The energy transfer to the Li-like ion of rest mass  $M_0$  is<sup>6</sup>  $\delta E_{\parallel} = \delta(\gamma M_0 c^2) = \beta \cdot \delta(\beta\gamma M_0 c) = \beta \cdot \overline{\delta p_{\parallel}} = \beta\gamma \hbar\omega_0/c$ , and the mean relative

<sup>4</sup> The subject of laser cooling for relativistic beams has been discussed by Habs et al. 1991 and for SIS300 recently by Schramm et al. 2004, and Schramm et al. 2006.

<sup>5</sup> This result can also directly be obtained by a Lorentz transformation of the transferred momentum  $\hbar\omega_0/c$  in the rest frame of the Li-like ion into the laboratory system.

<sup>6</sup> Also this relation follows directly from the Lorentz transformation formulas.

change of the relativistic factor at resonance absorption and re-emission of a single photon is given by

$$\frac{\delta\gamma}{\gamma} = \beta \frac{\hbar\omega_0}{M_0c^2} = (1 + \beta)\beta\gamma \frac{\hbar\omega_L}{M_0c^2} \cong 2\gamma \frac{\hbar\omega_L}{M_0c^2} . \quad (27)$$

The numerical result for Li-like uranium at  $\gamma = 25.68$  is  $\delta\gamma/\gamma = 1.27 \cdot 10^{-9}$ . A total energy shift  $\Delta\gamma_b/\gamma = 10^{-4}$  requires a small de-tuning of the laser frequency in such a manner that first only the ions with largest energies are optically pumped. These are shifted to lower energies by a gradual increase of the laser frequency. In this manner successively more and more ions of the bunch are included in the pumping process. For a complete cooling cycle at least a number  $(\Delta\gamma_b/\gamma)/(\delta\gamma/\gamma)$  of transitions is required.

The rate at which  $\gamma$  varies at saturation follows for a pulse laser system with pulse width  $\Delta t_{pulse}$  and repetition rate  $f_{rep}$  from equations (27) and (14) as

$$\dot{\gamma}|_{sat} = \frac{d\gamma/\gamma}{dt}|_{sat} = \beta \frac{\hbar\omega_0}{A \cdot m_u c^2} \frac{1}{2} \left( A_{ki} \frac{\Delta t_{pulse}}{\gamma} + 1 \right) \cdot f_{rep} . \quad (28)$$

Here  $A$  is the atomic number of the Li-like ion and  $m_u$  the atomic mass unit. With the numbers of our example the cooling rate is  $\dot{\gamma}/\gamma|_{sat} = 0.46 \cdot 10^{-4}/s$  for  $^{238}\text{U}$ . A lower limit for the corresponding cooling time is for  $\Delta\gamma_b/\gamma = 10^{-4}$

$$\tau_c = \frac{\Delta\gamma_b/\gamma}{\dot{\gamma}/\gamma|_{sat}} = 2.2 \text{ s} . \quad (29)$$

It might be of interest to know how the cooling rate varies as function of the charge number  $Z$ . For  $^{120}\text{Sn}$  ( $Z = 50$ ), as an example, one obtains with  $\hbar\omega_0 = 107.95$  eV and  $A_{ki} = 4.606 \cdot 10^9/s$ , both taken from Johnson et al.,  $\gamma = 25.68$ , and  $f_{rep} = 10$  kHz a  $\dot{\gamma}/\gamma|_{sat} = 0.135 \cdot 10^{-4}/s$ . However, cooling of Li-like Sn via the  $^2P_{3/2} - ^2S_{1/2}$  transition at  $\hbar\omega_0 = 374.70$  eV,  $A_{ki} = 2.057 \cdot 10^{11}/s$ , and an increased  $\gamma = 36$  results in a nearly two orders of magnitude faster rate  $\dot{\gamma}/\gamma|_{sat} = 9.74 \cdot 10^{-4}/s$ .

While in longitudinal direction the ions are cooled, they are heated in transverse direction. The variance of the transverse momentum transfer is given by

$$\overline{\delta p_{\perp}^2} = \int_{-1}^1 \frac{(\hbar\omega_0/c)^2 \sin^2 \Theta}{\gamma^2 (1 - \beta \cos \Theta)^2} \cdot \frac{1}{2} \frac{d(\cos \Theta)}{\gamma^2 (1 - \beta \cos \Theta)^2} = \frac{2}{3} \left( \frac{\hbar\omega_0}{c} \right)^2 . \quad (30)$$

Again, the integral has been solved analytically with the result given at the right hand side of equation (30)<sup>7</sup>. The angular spread is

$$\frac{\sqrt{\delta p_{\perp}^2}}{\beta\gamma M_0 c} = \sqrt{\frac{2}{3}} \cdot \frac{\hbar\omega_0}{\beta\gamma M_0 c^2} \quad (31)$$

with  $\beta\gamma M_0 c$  the momentum of the Li-like system. The total angular spread after a number of  $(\Delta\gamma_b/\gamma)/(\delta\gamma/\gamma)$  uncorrelated emissions of photons is

$$\sigma'_{HI} = \sqrt{\frac{\Delta\gamma_b/\gamma}{\delta\gamma/\gamma}} \sqrt{\frac{2}{3}} \cdot \frac{\hbar\omega_0}{\beta\gamma M_0 c^2}. \quad (32)$$

With the numbers of our example the result is  $\sigma'_{HI} = 0.0113 \mu\text{rad}$  which probably is negligibly small in comparison to the angular spread of the HI beam with an emittance of about  $1 \pi \text{ mm mrad}$ .

Since the energy spread after laser cooling is in the order  $\Delta\nu_L/\nu_L = 5.3 \cdot 10^{-7}$ , a superior line width in the hyperfine structure pattern can be expected with laser cooling.

## 6. Nuclear polarization by optical pumping

A few remarks will be added on the possibility to prepare a polarized Li-like ion beam which exhibits also a nuclear polarization if the nuclear spin is not zero. As schematically shown in figure 6, pumping with left-circularly polarized laser light results after many transitions finally in a population of only the  $|F = I + 1/2, M_F = -(I + 1/2)\rangle$  Zeeman level, because this level can not be pumped anymore. In this state the electronic spin as well as the nuclear spin are polarized as sketched schematically in the vector coupling model inset in figure 6.

Unfortunately, a polarization may probably not be maintained within the SIS300 ring since in the strong magnetic field of the bending magnets and beam optical elements a polarized total angular momentum  $\vec{F}$  precesses and may randomize. However, it might be conceivable that an external Li-like beam may be pumped in a long straight section, for instance by 100 ns long circularly polarized laser beams which would induce, according to equation (14),  $N_{0,sat} = 32$  transitions in an unpolarized Li-like ion. This is a rather large number and the attained polarization may already be high. For Li-like ions with  $Z \leq 50$ , it could be pumped via the much faster  ${}^2P_{3/2} - {}^2S_{1/2}$  transition and even much larger numbers may be attained at even shorter laser pulse durations.

<sup>7</sup> The integration may as well be performed in the rest frame of the Li-like system with the same result  $\overline{\delta p_{\perp}^2} = \int_{-1}^1 (\hbar\omega_0/c)^2 \cdot \sin^2 \Theta_0 \cdot (1/2) \cdot d(\cos \Theta_0) = (2/3)(\hbar\omega_0/c)^2$ .

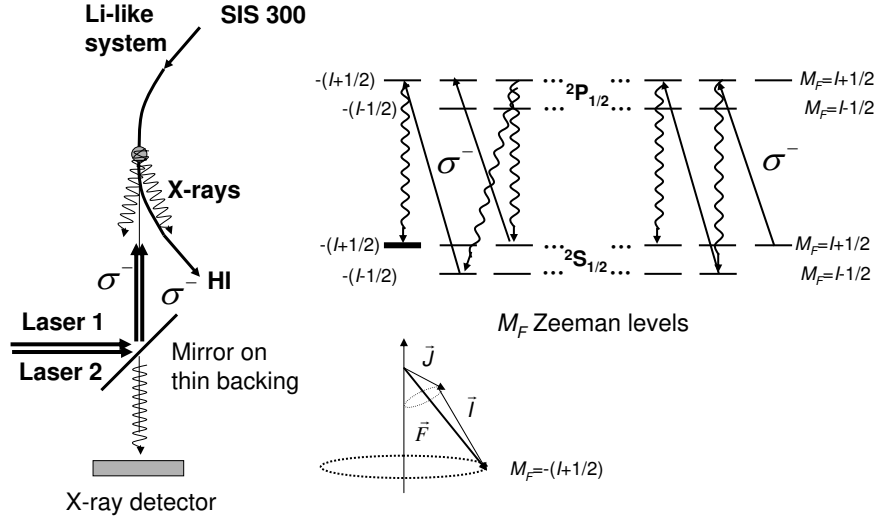


Figure 6. Scheme of the experimental setup for polarization of the Li-like ion beam (left), and pumping scheme with circularly polarized laser light (right). Shown are the Zeeman levels for the hyperfine levels of the ground and excited state with  $F = I \pm 1/2$ , with  $I$  the nuclear spin. After a very long pumping time only the  $F = -(I + 1/2)$  Zeeman level will be populated.

For quantitative numbers, however, detailed calculations are required which were beyond the scope of this work.

## 7. Conclusions

Precision transition energies  $\hbar\omega_0$  as well as relativistic factors  $\gamma$  can be measured for Li-like ions at the future heavy ion accelerator SIS300 if the inherently very precise laser spectroscopy method is combined with a precision X-ray energy measurement of fluorescence photons by means of a single crystal monochromator. Isotope shifts and magnetic moments can be measured at the  $^2P_{1/2} - ^2S_{1/2}$  transition for all elements, and quadrupole moments for  $Z \leq 50$  at the  $^2P_{3/2} - ^2S_{1/2}$  transition, in principle even at a single stored radioactive species far off stability if their nuclear spin is known. Heavy ion beams in SIS300 may be laser cooled, and polarized external heavy ion beams may be prepared by optical pumping with polarized laser beams.

## Acknowledgements

I thank Dr. W. Lauth, Dr. A. Wolf for fruitful discussions, Dr. P. Kunz for critical comments on the manuscript, and Dr. F. Hagenbuck for valuable information on SIS300.

This work has been supported by Bundesministerium für Bildung und Forschung under contract 06 MZ 169 I.

## References

- Backe, H. Laser Spectroscopy and cooling of relativistic ions. Talk presented at the GSI Workshop on its Future Facility, Darmstadt, Germany, October 18-20, 2000.
- Beiersdorfer, P. and Chen, H. and Thorn, D. B. and Träbert, E. Measurement of the Two-Loop Lamb Shift in Lithiumlike  $U^{89+}$ . *Phys. Rev. Lett.*, 95:233003-1–233003-4, 2005.
- Bosselmann, Ph., U. Staude, D. Horn, and K.-H. Schartner, F. Folkmann, A. E. Livingston, P. H. Mokler. Measurements of  $2s^2S_{1/2} - 2p^2P_{1/2,3/2}$  transition energies in lithiumlike heavy ions. II. Experimental results for  $Ag^{44+}$  and discussion along the isoelectronic series. *Phys. Rev. A*, 59:1874–1883, 1999.
- Boucard, S., and P. Indelicato. Relativistic many-body and QED effects on the hyperfine structure of lithium-like ions. *Eur. Phys. J. D*, 8:59–73, 2000.
- Brandau, C. and Kozhuharov, C. and Müller, A. and Shi, W. and Schippers, S. and Bartsch, T. and Böhm, S. and Böhme, C. and Hoffknecht, A. and Knopp, H. and Grün, N. and Scheid, W. and Steih, T. and Bosch, F. and Franzke, B. and Mokler, P. H. and Nolden, F. and Steck, M. and Stöhlker, T. and Stachura, Z. . Precise Determination of the  $2s_{1/2} - 2p_{1/2}$  Splitting in Very Heavy Lithiumlike Ions Utilizing Dielectronic Recombination. *Phys. Rev. Lett.*, 91:073202-1–073202-4, 2003.
- Caticha, Ariel. Transition-diffracted radiation and Cerenkov emission of x rays. *Phys. Rev. A*, 40:4322–4329, 1989.
- Gutbrod, H.H., K.-D. Groß, W.F. Henning, V. Metag. An International Accelerator Facility for Beams of Ions and Antiprotons. W.F. Henning (Editor in Chief). Conceptual Design Report, GSI, Darmstadt, 2001, p. 430.
- Gutbrod, H.H., I. Augustin, H. Eickhoff, K.-D. Groß, W. F. Henning, D. Kräamer, G. Walter. FAIR Baseline Technical Report. H.H. Gutbrod (Editor in Chief). <http://www.gsi.de/fair/reports/btr.html>, Volume 2 - Accelerator and Science Infrastructure, p. 43.
- Habs, D, V. Balykin, M. Grieser, R. Grimm, E. Jaeschke, M. Music, W. Petrich, D. Schwalm, A. Wolf, G. Huber, R. Neumann. RELATIVISTIC LASER COOLING. In R. Calabrese and L. Tecchio, editors, *Proceedings of the Workshop, 'ELECTRON COOLING and NEW COOLING TECHNIQUES'*, Legnaro, Padova, Italy, May 1990. World Scientific, Singapore, New Jersey, London, Hong Kong, p. 122.
- Johnson, W. R., Z. W. Liu, and J. Sapirstein. Transition rates for lithium-like ions, sodium-like ions, and neutral alkali-metal atoms. *Atomic Data and Nuclear Data Tables*, 64:279–300, 1996.

- Persson, H., I. Lindgren, S. Salomonson, P. Sunnergren. Accurate vacuum-polarization calculations. *Phys. Rev. A*, 48:2772–2778, 1993.
- Saathoff, G., S. Karpuk, U. Eisenbarth, G. Huber, S. Krohn, R. Muñoz Horta, S. Reinhardt, D. Schwalm, A. Wolf, and G. Gwinner. Improved Test of Time Dilation in Special Relativity. *Phys. Rev. Letters*, 91:190403-1–190403-4, 2003.
- Shabaev, V.M., M.B. Shabaeva, I.I. Tupitsyn and V.A. Yerokhin. Hyperfine structure of highly charged ions. *Hyperfine Interactions*, 114:129–133, 1998.
- Schramm, U., M. Bussmann, D. Habs. From laser cooling of non-relativistic to relativistic ion beams. *Nucl. Instr. and Meth. in Phys. Res. A*, 532:348–356, 2004.
- Schramm, U., M. Bussmann, D. Habs, T. Kühl, P. Beller, B. Franzke, F. Nolden, M. Steck, G. Saathoff, S. Reinhardt and S. Karpuk. Combined laser and electron cooling of bunched  $C^{3+}$  ion beams at the storage ring ESR. Proceedings of the International Conference ‘COOL2005’, Galena, USA, September 2005. *AIP Conf. Proceedings*, 821:501–509, 2006.
- Schweppe, J., A. Belkacem, L. Blumenfeld, Nelson Claytor, B. Feinberg, Harvey Gould, V. E. Kostroun, L. Levy, S. Misawa, J. R. Mowat, and M. H. Prior. Measurement of the Lamb shift in lithiumlike uranium ( $U^{89+}$ ). *Phys. Rev. Letters*, 66:1434–1437, 1991.
- Stepanov, Sergey. X-RAY SERVER. *www*, <http://sergey.gmca.aps.anl.gov/>.
- Yerokhin, V. A., A. N. Artemyev, V. M. Shabaev, M. M. Sysak, O. M. Zhrebtsov, and G. Soff. Evaluation of the two-photon exchange graphs for the  $2p_{1/2} - 2s$  transition in Li-like ions. *Phys. Rev. A*, 64:032109-1–032109-15, 2001.
- Yerokhin, V. A. private communication.
- Ynnermann, A., J. James, I. Lindgren, H. Persson, S. Salomonson. Many-body calculations of the  $2p_{1/2,3/2} - 2s_{1/2}$  transition energies in Li-like  $^{238}\text{U}$ . *Phys. Rev. A*, 50:4671–4678, 1994.